TITLE

Targeting T-cell receptor β-constant for immunotherapy of T-cell malignancies

AUTHORS

Paul M. Maciocia[1], Patrycja A. Wawrzyniecka[1], Brian Philip[1], Ida Ricciardelli[2], Ayse U. Akarca[1], Shimobi Onuoha[3], Mateusz Legut[4], David K. Cole[4], Andrew K. Sewell[4], Giuseppe Gritti[5], Joan Somja[6], Miguel A. Piris[7], Karl S. Peggs[1], David C. Linch[1], Teresa Marafioti[1], Martin A. Pule[1,3]*

[1] University College London, Cancer Institute, London, UK

[2] University College London, Institute of Child Health, London, UK

[3] Autolus Ltd, London, UK

[4] Division of Infection and Immunity, Cardiff University School of Medicine, UK

[5] Department of Haematology, Papa Giovanni XXII Hospital, Milan, Italy

[6] Department of Anatomy and Cellular Pathology, University of Liege, Belgium

[7] Anatomical Pathology Service, University Hospital Marques de Valdecilla (IFIMAV), Santander, Spain

* Corresponding author

ACKNOWLEDGEMENTS

PM was supported by a studentship from Cancer Research UK. M. Pule and TM are supported by the UK National Institute of Health Research University College London Hospital Biomedical Research Centre. AA and ML are supported by Cancer Research UK. DKC is a Wellcome Trust Career Development Fellow. AKS is a Wellcome Trust Senior investigator. This project is supported by grants from the Kay Kendall Leukaemia Fund and Innovate UK. We would like to thank Dr Michael Owen and Dr Joanne Viney for helpful discussions.

CONTRIBUTIONS

PM designed and performed the experimental work and wrote the manuscript. PW performed experimental work. BP designed and performed *in vivo* experiments, and wrote the manuscript. IR generated and tested EBV-CTLs. AA performed immunohistochemistry. SO, DC and AS produced soluble TCR molecules, performed surface plasmon resonance analysis and wrote the manuscript. ML and AK identified and characterised iNKTs. GG, JS and M.Piris supplied clinical samples. KP and DL helped design experiments and wrote the manuscript. TM optimised and analysed immunohistochemical staining, and wrote the manuscript. M.Pule conceived the idea, designed the experimental work and wrote the manuscript.

ABSTRACT

Mature T-cell cancers are typically aggressive, treatment-resistant and associated with poor prognosis. Translation of immunotherapeutic approaches has been limited by a lack of target antigens discriminating malignant from healthy T-cells. Unlike B-cell depletion, pan T-cell aplasia is prohibitively toxic. We report a novel targeting strategy based on the mutually exclusive expression of either *TRBC1* or *TRBC2* T-cell receptor (TCR) β-constant domain. We identify an antibody with unique TRBC1 specificity, and use this to rapidly screen for T-cell clonality, demonstrating that while normal and viral-specific T-cells contain TRBC1 and TRBC2 compartments, malignancies are restricted to only one. As proof of concept for anti-TRBC immunotherapy, we developed anti-TRBC1 CART-cells, which recognise and kill normal and malignant TRBC1 but not TRBC2 T-cells, *in vitro* and in a disseminated murine leukaemia model. Unlike non-selective approaches targeting the entire T-cell population, TRBC-targeted immunotherapy could eradicate a T-cell malignancy while preserving sufficient normal T-cells to maintain cellular immunity.

INTRODUCTION

Mature T-cell lymphomas (PTCLs) are a heterogeneous group of disorders, collectively comprising 10-15% of non-Hodgkin's lymphoma[1]. These cancers typically behave aggressively[2,3]. Outcomes are worse than equivalent B-cell cancers, with an overall estimated 5-year survival of only 32%[3]. Furthermore, while treatment of B-cell cancers benefits from targeted immunotherapies such as therapeutic monoclonal antibodies (mAbs)[4], bispecific T-cell engagers[5] and more recently chimeric antigen receptor (CAR) T-cell therapy[6,7], no such approaches are available for T-cell cancers.

Immunotherapies used in B-cell malignancies target pan B-cell antigens, since no antigens exist which discriminate normal from malignant B-cells. The consequent depletion of the normal B-cell compartment is surprisingly well tolerated and is considered an acceptable side-effect[6,7]. The situation is different with T-cells: once again, no antigens exist which discriminate normal from malignant T-cells[3,8]; however, T-cell aplasia consequent to targeting a pan T-cell antigen would lead to profound and unacceptable immunosuppression[9]. Here, we describe a targeting approach for treating mature T-cell cancers which relies on recognition of a pan T-cell antigen, but avoid severe immunosuppression.

The α/β T-cell receptor (TCR) is a pan T-cell antigen. Apart from its expression on normal T-cells it is an ideal target: it is expressed by >95% of cases of PTCL-NOS[8], almost all AITL[8], as well as 30% of T-acute lymphoblastic leukaemia (T-ALL)[10]. High and homogenous surface expression is commonly seen on lymphoma cells[11] and in addition, evidence exists that a proportion of PTCL cases may depend on TCR-associated signalling for lymphomagenesis and survival[12]. TCR α and β chains comprise amino-terminal variable and carboxy-terminal constant regions[13] (Figure 1a). TCR diversity is generated by somatic recombination, when each TCR chain selects a variable (V), diversity (D), joining (J) and constant (C) region[13]. Importantly, cells of a clonal T-cell population all express the same unique TCR. However, approaches targeting TCR variable regions unique to a malignant clone are impracticable, since a bespoke therapeutic is required for each patient.

An oft-forgotten feature of TCR β-chain recombination is that there are two β-constant region genes: TRBC1 and TRBC2. Each TCR (and therefore each T-cell) expresses, mutually exclusively and irreversibly, TCR β-constant coded by either TRBC1 or TRBC2[14,15] (Figure 1b). Hence, normal T-cells will be a mixture of individual cells

expressing either TRBC1 or 2, while a T-cell cancer will express either TRBC1 or 2 in its entirety. We propose targeting TRBC1 in case of a TRBC1+ T-cell malignancy, or the converse in case of a TRBC2+ malignancy. This will target all cells of the malignant clone, but leave a substantial proportion of the T-cell compartment intact.

In this work, we demonstrate that it is possible to distinguish between TRBC1 and 2 TCRs with an antibody, despite almost identical amino acid sequences (Figure 1c). We show that peripheral blood T-cells in normal subjects comprise of a mixture of approximately 35:65% TRBC1/2 cells, and that complete depletion of either TRBC1 or 2 compartments will still maintain adequate viral immunity. We confirm TRBC clonality in many types of T-cell malignancies by both flow cytometry and immunohistochemistry. Finally, we demonstrate efficacy of a CAR with TRBC1 specificity to prove our targeting concept.

RESULTS

JOVI-1 mAb is specific for TRBC1-expressing cells

To find a TRBC specific binder, we screened anti-TCR mAbs which are known to bind a proportion of T-cells in peripheral blood. In order to screen for TRBC1/2 specificity we cloned the α and β-chains of the well-characterised HA-1 TCR[16] in TRBC2 (native) format or with mutations introduced in the constant domain to convert to TRBC1. We stably expressed either TCR on the surface of Jurkat T-cell line with knocked out TCR α and β loci (JKO). Analysis by flow cytometry demonstrated that, while both TRBC1-JKO and TRBC2-JKO lines expressed surface TCR/CD3, mAb JOVI-1[17] recognised only TRBC1-JKO cells and not TRBC2-JKO cells (Figure 1d), confirming the TRBC1 specificity of this antibody. Surface plasmon resonance analysis demonstrated that JOVI-1 bound to a TRBC1-TCR with an affinity of K_D = 0.42nM and a half-life of ~30mins, in line with other therapeutic antibodies[18]. In contrast, JOVI-1 binding to a TRBC2-TCR was >10,000x weaker, demonstrating the remarkable specificity of the reagent (supplementary Figure 1).

TCR β-junctional regions segregate with constant domains: TCRs selecting TRBJ1 1-6 use TRBC1, and those selecting TRBJ2 1-7 use TRBC2[13]. It was therefore possible that JOVI-1 only maintains TRBC1-specificity in the context of particular junctional regions. We cloned several TCRs of varying antigen specificity, utilising a range of variable/ junctional regions, from publicly available sequences. When transfected into human embryonic kidney (HEK)-293T cells along with a plasmid supplying the components of CD3, TCRs were expressed on the cell surface. JOVI-1 uniformly recognised TRBC1 cells despite varying TRBJ1 regions, and did not recognise cells expressing TRBC2 TCRs and varying TRBJ2 regions (Figure 1e). In addition, we cloned a truncated TCR lacking α and β V(D)J domains. CD3 staining confirmed surface assembly, and staining with JOVI-1 was similar to that seen with full-length TCR (Figure 1f). This offered further confirmation that junctional regions were not required for the JOVI-1 epitope.

We then sought to determine the residues of TRBC responsible for the TRBC1-specificity of JOVI-1. Structural analysis suggested that the F->Y at residue 36 is buried in secondary structure and V->E at residue 135 is likely too close to the membrane to be accessible. However, the NK->KN difference at residues 4-5 is exposed to the surface and represents a substantial difference of both shape and

charge to the epitope. By introducing each mutation required to convert TRBC2 to TRBC1 individually, we confirmed that the reversal of asparagine and lysine residues at positions 3-4 was indeed the discriminating portion of the JOVI-1 epitope (Figure 1f,g).

Normal αβ T-cells contain a mixture of TRBC1+ and TRBC1- populations

Using JOVI-1, we then sought to determine the proportion of T-cells from normal donors that were TRBC1 versus TRBC2. Each donor had TCR+TRBC1+ and TCR+TRBC1- cells in both CD4 and CD8 compartments, with median TRBC1 expression of 35% (range 25-47%, Figure 2a,b). We also confirmed that CD4 and CD8 differentiation subsets all contained both populations with a similar TRBC1:TRBC2 ratio (Suppl Fig 2a,d). In addition, we identified 2 cell types which express a semi-invariant restricted TCR repertoire, mucosal-associated invariant T-cells (MAITs, suppl Fig 2b,d) and invariant natural killer/ T-cells (iNKTs, suppl Fig 2c,d) and demonstrated that these populations also contain both TRBC1+ and TRBC1- cells, albeit with a lower TRBC1 proportion than seen in bulk T-cell populations.

Although the polyclonal T-cell population in normal donors contained both TRBC1 and TRBC2 cells, we reasoned that the T-cell response to a particular virus may be skewed towards one of these, and therefore that removal of one subset could result in loss of cellular immunity. To determine if this was the case, we generated oligoclonal Epstein Barr Virus (EBV)-specific cytotoxic T-cell lines from normal donors, as previously described[19]. These cells lysed autologous EBV-transformed cells (Figure 2c). Staining in 3 donors revealed the cells were >98% CD8+ (data not shown) and contained a mixed population of TRBC1+ and TRBC1- (median 45% TRBC1+) cells, demonstrating that the T-cell response to EBV contains both populations (Figure 2d). In addition, we identified T-cells specific for cytomegalovirus (CMV) or adenovirus (AdV) by incubation of peripheral blood mononuclear cells (PBMCs) with pools of antigenic peptides. Viral-specific T-cells, identified by interferon-gamma (IFN-γ) expression after peptide incubation (Figure 2e), were found to contain both TRBC1+ and TRBC1- cells (Figure 2f). Summary data from normal donors demonstrated median TRBC1 expression of 45% (CMV) and 41% (AdV) (Figure 2g).

T-cell derived malignant cell lines and primary T-cell tumours are clonally TRBC1+ or TRBC1-

Surface TCR+ cell lines were stained with JOVI-1 and were found to be either TRBC1+ (H9, Jurkat, MJ) or TRBC1- (HD-Mar2, HPB-ALL, T-ALL1, HH, T-ALL1). TRBC1 versus TRBC2 expression was confirmed at the transcriptional level by PCR amplification of the β-constant region from cDNA, followed by Sanger sequencing (Figure 3a). These data confirmed JOVI-1 as a marker of TRBC1 clonality in cell lines. Next, using multiparameter flow cytometry, we analysed primary blood samples from several patients with T-large granular leukaemia (T-LGL), a TCR+ lymphoproliferative disorder characterised by circulating tumour cells which express CD57[20]. While CD57+ tumour cells demonstrated markedly skewed TRBC1:TRBC2 ratios, normal CD4+ and CD8+ T-cells displayed appropriate ratios of each population (Figure 3b). Using intracellular staining, we replicated this finding in primary marrow samples of T-ALL (Figure 3c). Further, using flow cytometry (FACS) or immunohistochemistry (IHC) on frozen tissue sections, we stained a number of primary samples of TCR+ malignancies of multiple histologies and confirmed that TRBC1 staining could be used to determine if tumours were clonally TRBC1+ or TRBC1- (Figure 3d,e). In 58 samples (38 analysed by IHC, 20 by FACS), 40% were TRBC1+ and 60% were TRBC1- (Figure 3f). Of note, TCR/CD3 expression assayed by FACS in primary tumours was typically at a similar level to admixed normal T-cells (median MFI = 96% of normal T-cell MFI), other than in adult T-cell leukaemia/ lymphoma (ATLL) where expression was typically dimmer than in normal T-cells (median MFI 23% of normal T-cell MFI, Fig 3g).

T-cells transduced with anti-TRBC1 CAR specifically target TRBC1+ but not TRBC2+ cells *in vitro*

As a proof of concept for therapies targeting TRBC we cloned a single-chain variable fragment based on the JOVI-1 antibody into a 3rd generation CAR format[21]. We retrovirally transduced T-cells from normal donors to stably express this construct, and confirmed surface expression of CAR on up to 90% of cells (Fig 4a). We subsequently co-cultured non-transduced (NT) or anti-TRBC1 CAR T-cells with NT-JKO, TRBC1-JKO or TRBC2-JKO cells. While NT effectors did not secrete IFN-γ in response to any target cells, TRBC1 CAR T-cells specifically released IFN-γ only when incubated with TRBC1-JKO and not NT-JKO or TRBC2-JKO cells (Figure 4b,c). In 4hr chromium release cytotoxicity assays, NT cells did not display cytotoxicity, while anti-TRBC1

CAR T-cells specifically killed TRBC1-JKO and not NT-JKO or TRBC2-JKO cells (Figure 4d,e).

In addition, we performed flow cytometric cytotoxicity assays using multiple α/ β TCR+ cell lines as targets, and confirmed killing of TRBC1+ but not TRBC2+ cell lines by anti-TRBC1 CAR T-cells, while NT T-cells did not lyse either (Figure 4f). Next, to simulate a physiological setting, we mixed TRBC1-JKO cells labelled with CD19 marker gene at 1:1 ratio with TRBC2-JKO cells labelled with blue fluorescent protein (BFP). This population was co-cultured with anti-TRBC1 CAR-T or NT cells. Analysis at 48hrs confirmed eradication of TRBC1 cells with preservation of TRBC2 cells by anti-TRBC1 CAR, and no killing of either population seen with NT effectors (Figure 4g).

We obtained primary tumour cells from multiple patients with TRBC1+ T-cell malignancies. We co-cultured patient tumour with NT or anti-TRBC1 CART-cells at a 1:1 ratio. Using allogeneic T-cells, we demonstrated specific kill of tumour in cases of T-prolymphocytic leukaemia (T-PLL) and PTCL-NOS, with preservation of a substantial proportion of residual normal T-cells (Figure 4h). Tumour kill was seen even in cases of ATLL (Figure 4i,l), where TCR/CD3 was partially downregulated from the cell surface (Figure 2g). In addition, we demonstrated successful transduction of T-cells from a patient with TRBC1+ malignancy (ATLL) despite heavy circulating tumour burden (Figure 4j), that the T-cell product was 'purged' of contaminating tumour cells (Figure 4k) and that anti-TRBC1 CAR specifically killed autologous tumour cells (Figure 4l).

Anti-TRBC1 CAR-T cells selectively deplete normal TRBC1, but not TRBC2 cells

Following anti-TRBC1 CAR transduction, no TRBC1+ cells could be detected in either the transduced or non-transduced fractions, indicating possible depletion of this population (Suppl Fig 3a). However, we reasoned that absent TRBC1 staining was likely due to epitope blocking by ligated anti-TRBC1 CAR. Therefore, we transduced cells with anti-TRBC1 CAR and CD34 marker gene[22]. This enabled sorting of cells into CAR+ and CAR- fractions using CD34-bead magnetic depletion. We confirmed depletion of all CAR+ cells in the –ve fraction, thus excluding any effect of epitope blockade by CAR. While NT cells contained both TRBC1+ and TRBC1- fractions, the CAR –ve fraction did not contain any TRBC1+ cells, confirming selective depletion of TRBC1 cells (Suppl Figure 3b). Further, we sorted normal donor T-cells into TRBC1+

and TRBC1- populations using magnetic beads. We subsequently separately labelled each population with different fluorescent nuclear dyes, enabling later discrimination of the populations, and co-cultured with autologous NT or anti-TRBC1 CART-cells. While TRBC2 cells co-cultured with anti-TRBC1 CAR were not depleted compared to NT condition, TRBC1 cells were 80% depleted at 7 days (Suppl Figure 3c), indicating selective purging of this population. This was confirmed in a further assay, in which TRBC1 cells were mixed at a 1:2 (physiological) ratio with TRBC2 cells before 1:1 co-culture with NT or anti-TRBC1 cells. At 7 days, virtually all TRBC1 cells had been depleted from the culture, while TRBC2 cells remained (Suppl Fig 3d). Finally, to further mitigate against potential transduction of contaminating TRBC1 tumour cells, we pre-depleted normal donor T-cells of TRBC1+ cells to obtain cells which were >99% TRBC1- (Supplementary Figure 3e), then demonstrated transduction with anti-TRBC1 CAR that was similar to that achieved for unsorted cells (Supplementary Figure 3f).

Anti-TRBC1 CAR-T cells specifically killed TRBC1+ tumour while preserving TRBC2+ tumour in murine models of disseminated T-cell malignancy.

We utilised an established murine xenograft model of disseminated T-cell leukaemia. Non-obese diabetic-severe combined immunodeficiency γ-chain–deficient (NSG) mice (Jackson) were intravenously injected with Jurkat T-cells, which natively express a TRBC1 TCR at a level similar to primary tumour and normal T-cells (Figure 2g). Jurkat cells were modified to stably express firefly luciferase (F-Luc) and CD19 marker gene, and stably engrafted in the bone marrow of all injected animals by day 6 (Figure 5a,b). Following engraftment, we treated mice with T-cells expressing anti-TRBC1 CAR or a control (irrelevant) CAR. Mice treated with anti-TRBC1 CAR had dramatic tumour reduction by BLI at D10 (Figure 5b,c), and this was associated with a substantial survival benefit. In a further experiment to evaluate CAR persistence (Figure 5e), we demonstrated tumour clearance and increased numbers of anti-TRBC1 versus control CAR T-cells in peripheral blood at D21 following T-cell injection (Figure 5f). Bone marrow was harvested at the time of death (survivors culled at D42), with similar results seen (Figure 5g).

Next, we injected a further cohort of mice with equal proportions of Jurkat-TRBC1 cells (human CD19 marker gene) and JKO cells engineered to express TRBC2 TCR and BFP marker gene). Tumour engraftment in marrow was confirmed in all animals by BLI at day 6. Animals were then treated with NT or anti-TRBC1 CAR T-cells. Flow

cytometry of bone marrow confirmed the TRBC1 specificity of anti-TRBC1 CAR T-cells *in vivo*: while mice receiving NT effectors had approximately equal proportions of Jurkat-TRBC1 and JKO-TRBC2 cells in marrow, only JKO-TRBC2 cells were seen in recipients of anti-TRBC1 CAR T-cells (Figure 5e,f).

Finally, in order to determine if anti-TRBC1 CAR was able to deplete TRBC1 tumour in a physiological setting (ie in the presence of normal T-cells), we engrafted NSG mice with Jurkat-CD19-Fluc tumour as before. After 7 days, mice were injected with human PBMCs (Supplementary Fig 4a). After a further 7 days, human monocyte and T-cell engraftment was confirmed by flow cytometry of peripheral blood (Supplementary Fig 4b), and progressive disease was demonstrated by BLI (Supplementary Fig 4c). Animals were then injected with anti-TRBC1 CAR or control CAR, with cells prepared from the same donor as initial PBMCs. BLI and flow cytometry of bone marrow at 5 days following treatment demonstrated tumour control in anti-TRBC1 CAR recipients, but disease progression in control CAR recipients (Supplementary Fig 4c,d,e). Flow cytometry of bone marrow (Supplementary Figure 4e) and spleen (Supplementary Figure 4f) at D6 demonstrated similar numbers of non-CAR T-cells were present in anti-TRBC1 and control CAR recipients, confirming persistence of normal T-cells in the face of tumour depletion.

DISCUSSION

The presence of two functionally identical genes at the TCR-β constant region has been recognised for more than 30 years[14,15], but has not been exploited until now. We have demonstrated that despite highly similar amino acid sequences, it is possible to discriminate between TRBC1 and TRBC2 proteins on normal and malignant T-cells. Indeed, JOVI-1 demonstrated >10,000-fold difference in binding affinity, with specificity based on the reversal of only 2 residues in TRBC. Consistent with previous findings, we have shown that approximately 2/3 of both normal T-cells[23,24] and T-cell cancers[25] express TRBC2-TCR.

We believe TRBC1/2 targeting has considerable potential for immunotherapy of T-cell malignancies. The principle of using immunotherapy to target a rearranged clone-specific receptor is not new: Stevenson *et al* pioneered the use of patient-specific anti-idiotype mAbs against neoplastic lymphoma cells[26,27]. However, this approach is impracticable since it requires a novel binder to be generated for each patient. An analogous approach to ours, targeting B-cell cancers with antibody light-chain specific therapy has also been proposed[28].

Patients with B-cell malignancies have greatly benefited from the advent of potent immunotherapies. Rituximab, usually given in combination with cytotoxic chemotherapy, has dramatically improved outcomes in indolent[29] and aggressive B-cell lymphomas[30] and is now part of standard front-line therapy. Further agents including depleting antibodies, radio-immune conjugates, bi-specific T-cell engagers and other modalities have also proven effective and are in widespread use[31]. Of immunotherapies in development, perhaps the most promising approach is CAR T-cells. Treatment of B-cell malignancies with anti-CD19 CART-cells has been one of the most important recent advances in the treatment of cancer, with sustained remissions obtained in most patients with advanced and refractory B-ALL[6,32], as well as impressive though lesser responses in CLL[7,33] and diffuse large B-cell lymphoma[7]. Given the relatively similar presentation and nature of B- and T-cell malignancies, CART-cells could potentially have similar value in treating T-cell lymphomas.

However, anti-CD19 CART efficacy is accompanied by loss of the normal B-cell compartment[6,7]. While this is relatively well tolerated, and impact can be lessened by infusion of donor–derived pooled immunoglobulins, analogously targeting a pan-T-cell

antigen on a T-cell malignancy (with concomitant permanent loss of normal T-cells) would be prohibitively toxic, with no mitigating replacement therapies available.

Approaches using CARs against T-cell targets such as the pan T-cell antigen CD5[34] or CD4, which is present on a crucial subset of normal T-cells[35], have been proposed, but may prove unacceptably immunosuppressive in clinical use. With our approach, a patient treated with anti-TRBC1 CART would retain approximately 2/3 of normal T-cells, with polyclonal anti-viral immunity likely preserved. In addition, the potential for 'on-target off-tumour' toxicity affecting other tissues would be negligible, given the restriction of TCR expression to mature T- or NK/T-cells. However, with any approach targeting T-cells rather than B-cells increased cytokine-mediated toxicity could occur, due to lysis of normal tissue-resident T-cells and subsequent mediator release. Another potential consequence of depletion of part of the regulatory T-cell repertoire could be loss of some peripheral tolerance, if the T-regulatory cells protecting a particular tissue were particularly skewed towards TRBC1 or 2. However, ultimately the toxicities associated with depletion of TRBC1 or 2 cells could only be examined in a clinical trial.

In summary, we have demonstrated a novel approach to investigation and targeting of T-cell malignancies by distinguishing between two possible TCR beta-chain constant regions. Using CART-cells targeting one constant region we have demonstrated proof of concept. Exploration of the distribution of constant region usage by unselected normal T-cells and those providing specific viral immunity suggests that such an approach would not lead to significant immunosuppression. We hope that this approach heralds the application of potent targeted immunotherapeutics to provide much needed enhancement of the treatment of T-cell malignancies.

REFERENCES

1. A clinical evaluation of the International Lymphoma Study Group classification of non-Hodgkin's lymphoma. The Non-Hodgkin's Lymphoma Classification Project. *Blood* **89,** 3909–3918 (1997).
2. Vose, J., Armitage, J., Weisenburger, D.International T-Cell Lymphoma Project. International peripheral T-cell and natural killer/T-cell lymphoma study: pathology findings and clinical outcomes. *Journal of Clinical Oncology* **26,** 4124–4130 (2008).
3. Weisenburger, D. D. *et al.* Peripheral T-cell lymphoma, not otherwise specified: a report of 340 cases from the International Peripheral T-cell Lymphoma Project. *Blood* **117,** 3402–3408 (2011).
4. Gao, G. *et al.* A systematic review and meta-analysis of immunochemotherapy with rituximab for B-cell non-Hodgkin's lymphoma. *Acta Oncol* **49,** 3–12 (2010).
5. Bargou, R. *et al.* Tumor regression in cancer patients by very low doses of a T cell-engaging antibody. *Science* **321,** 974–977 (2008).
6. Maude, S. L. *et al.* Chimeric Antigen Receptor T Cells for Sustained Remissions in Leukemia. *N Engl J Med* **371,** 1507–1517 (2014).
7. Kochenderfer, J. N. *et al.* Chemotherapy-refractory diffuse large B-cell lymphoma and indolent B-cell malignancies can be effectively treated with autologous T cells expressing an anti-CD19 chimeric antigen receptor. *Journal of Clinical Oncology* **33,** 540–549 (2015).
8. Went, P. *et al.* Marker expression in peripheral T-cell lymphoma: a proposed clinical-pathologic prognostic score. *Journal of Clinical Oncology* **24,** 2472–2479 (2006).
9. Notarangelo, L. D., Kim, M.-S., Walter, J. E. & Lee, Y. N. Human RAG mutations: biochemistry and clinical implications. *Sci Rep* 1–13 (2016). doi:10.1038/nri.2016.28
10. Pui, C. H. *et al.* Heterogeneity of presenting features and their relation to treatment outcome in 120 children with T-cell acute lymphoblastic leukemia. *Blood* **75,** 174–179 (1990).
11. Jamal, S. *et al.* Immunophenotypic analysis of peripheral T-cell neoplasms. A multiparameter flow cytometric approach. *Am. J. Clin. Pathol.* **116,** 512–526 (2001).
12. Palomero, T. *et al.* Recurrent mutations in epigenetic regulators, RHOA and FYN kinase in peripheral T cell lymphomas. *Sci Rep* **46,** 166–170 (2014).
13. Delves, P. J., Martin, S. J. & Roitt, D. R. B. A. I. M. Roitt's Essential Immunology. 1–562 (2011).
14. Sims, J. E., Tunnacliffe, A., Smith, W. J. & Rabbitts, T. H. Complexity of human T-cell antigen receptor beta-chain constant- and variable-region genes. *Nature* **312,** 541–545 (1984).
15. Tunnacliffe, A., Kefford, R., Milstein, C., Forster, A. & Rabbitts, T. H. Sequence and evolution of the human T-cell antigen receptor beta-chain genes. *Proc. Natl. Acad. Sci. U.S.A.* **82,** 5068–5072 (1985).
16. Dickinson, A. M. *et al.* In situ dissection of the graft-versus-host activities of cytotoxic T cells specific for minor histocompatibility antigens. *Nat. Med.* **8,** 410–414 (2002).
17. Viney, J. L., Prosser, H. M., Hewitt, C. R., Lamb, J. R. & Owen, M. J. Generation of monoclonal antibodies against a human T cell receptor beta chain expressed in transgenic mice. *Hybridoma* **11,** 701–713 (1992).
18. Reff, M. E. *et al.* Depletion of B cells in vivo by a chimeric mouse human monoclonal antibody to CD20. *Blood* **83,** 435–445 (1994).
19. Ricciardelli, I. *et al.* Towards gene therapy for EBV-associated posttransplant

lymphoma with genetically modified EBV-specific cytotoxic T cells. *Blood* **124,** 2514–2522 (2014).

20. Swerdlow, S. H., International Agency for Research on CancerWorld Health Organization. *WHO Classification of Tumours of Haematopoietic and Lymphoid Tissues*. (International Agency for Research on Cancer, 2008).
21. Pule, M. *et al.* A chimeric T cell antigen receptor that augments cytokine release and supports clonal expansion of primary human T cells. *Molecular Therapy* **12,** 933–941 (2005).
22. Philip, B. *et al.* A highly compact epitope-based marker/suicide gene for easier and safer T-cell therapy. *Blood* **124,** 1277–1287 (2014).
23. Freeman, J. D., Warren, R. L., Webb, J. R., Nelson, B. H. & Holt, R. A. Profiling the T-cell receptor beta-chain repertoire by massively parallel sequencing. *Genome Research* **19,** 1817–1824 (2009).
24. Rosenberg, W. M., Moss, P. A. & Bell, J. I. Variation in human T cell receptor V beta and J beta repertoire: analysis using anchor polymerase chain reaction. *Eur. J. Immunol.* **22,** 541–549 (1992).
25. Brüggemann, M. *et al.* Powerful strategy for polymerase chain reaction-based clonality assessment in T-cell malignancies Report of the BIOMED-2 Concerted Action BHM4 CT98-3936. *Leukemia* **21,** 215–221 (2006).
26. Stevenson, F. K. *et al.* Antibodies to shared idiotypes as agents for analysis and therapy for human B cell tumors. *Blood* **68,** 430–436 (1986).
27. Hamblin, T. J. *et al.* Initial experience in treating human lymphoma with a chimeric univalent derivative of monoclonal anti-idiotype antibody. *Blood* **69,** 790–797 (1987).
28. Ramos, C. A. *et al.* Clinical responses with T lymphocytes targeting malignancy-associated κ light chains. *J. Clin. Invest.* **126,** 1–9 (2016).
29. Schulz, H. *et al.* Chemotherapy plus Rituximab versus chemotherapy alone for B-cell non-Hodgkin's lymphoma. *Cochrane Database Syst Rev* CD003805 (2007). doi:10.1002/14651858.CD003805.pub2
30. Fang, C., Xu, W. & Li, J.-Y. A systematic review and meta-analysis of rituximab-based immunochemotherapy for subtypes of diffuse large B cell lymphoma. *Ann Hematol* **89,** 1107–1113 (2010).
31. Boyiadzis, M. *et al.* The Society for Immunotherapy of Cancer consensus statement on immunotherapy for the treatment of hematologic malignancies: multiple myeloma, lymphoma, and acute leukemia. *Journal for ImmunoTherapy of Cancer* 1–25 (2016). doi:10.1186/s40425-016-0188-z
32. Davila, M. L. *et al.* Efficacy and toxicity management of 19-28z CAR T cell therapy in B cell acute lymphoblastic leukemia. *Sci Transl Med* **6,** 224ra25–224ra25 (2014).
33. Porter, D. L., Levine, B. L., Kalos, M., Bagg, A. & June, C. H. Chimeric antigen receptor–modified T cells in chronic lymphoid leukemia. *N Engl J Med* **365,** 725–733 (2011).
34. Mamonkin, M., Rouce, R. H., Tashiro, H. & Brenner, M. K. A T-cell-directed chimeric antigen receptor for the selective treatment of T-cell malignancies. *Blood* **126,** 983–992 (2015).
35. Pinz, K. *et al.* Preclinical targeting of human T-cell malignancies using CD4-specific chimeric antigen receptor (CAR)-engineered T cells. *Leukemia* **30,** 701–707 (2016).
36. Boulter, J. M. *et al.* Stable, soluble T-cell receptor molecules for crystallization and therapeutics. *Protein Eng.* **16,** 707–711 (2003).
37. Garboczi, D. N. *et al.* Assembly, specific binding, and crystallization of a human TCR-alphabeta with an antigenic Tax peptide from human T lymphotropic virus type 1 and the class I MHC molecule HLA-A2. *J. Immunol.* **157,** 5403–5410 (1996).
38. Wyer, J. R. *et al.* T cell receptor and coreceptor CD8 alphaalpha bind peptide-

MHC independently and with distinct kinetics. *Immunity* **10,** 219–225 (1999).
39. Straathof, K. C. An inducible caspase 9 safety switch for T-cell therapy. *Blood* **105,** 4247–4254 (2005).

OUTLINE METHODS

Cell lines

293T and K562 cell lines were cultured in IMDM (Lonza, Basel, Switzerland) supplemented with 10% FBS (FBS, HyClone, GE, Buckinghamshire, UK) and 2 mM GlutaMax (Invitrogen, CA, USA). Jurkat, Jurkat TCR-KO (and engineered variants), HD-Mar2, HPB-ALL, H9, T-ALL1, MJ, CCRF-CEM and HH cells were cultured in complete RPMI (RPMI1640, Lonza, Basel, Switzerland, supplemented with 10% FBS and 2 mM GlutaMax). Cells were maintained in a humidified atmosphere containing 5% CO2 at 37°C. All cell lines were routinely tested for mycoplasma and for surface expression of target antigens. All cell lines were obtained from American Tissue Culture Collection (ATCC), Deutsche Sammlung von Mikroorganismen und Zellkulturen (DSMZ) or Public Heath England collections. Jurkat TCR-KO cells were a kind gift from the laboratory of Prof Hans Stauss.

Cloning, expression and purification of TCR protein.

The C5861 TCR expressing a TRBC2 domain[36] and the ILA1 TCR expressing a TRBC1 domain[37], constructed using a disulphide-linked construct, were used to produce the soluble α- and β- chain domains (variable and constant) for each TCR. The TCRα and TCRβ chains were inserted into separate pGMT7 expression plasmids under the control of the T7 promoter. Competent Rosetta DE3 *E. Coli* cells (Merck, Darmstadt, Germany) were used to produce the C5861 and ILA1 TCRs in the form of inclusion bodies using 0.5M IPTG to induce expression. Soluble C5861 and ILA1 TCRs were refolded as previously described[36] purified by anion exchange (Poros 50HQ, Life Technologies, Cheshire, UK) and size exclusion chromatography (S200 GR, GE Healthcare, Buckinghamshire, U.K.).

Surface Plasmon Resonance (SPR) analysis

The binding analysis was performed using a Biacore T200 (GE Healthcare, Buckinghamshire, UK) equipped with a CM5 sensor chip as previously reported[38]. Briefly, 500-1000 Response Units (RUs) of JOVI-1 antibody was linked by amine coupling to the chip surface. For the C5861 TRBC2 TCR, ten serial dilutions were injected over the immobilised JOVI-1 and equibilibrium binding analysis was

545 performed. The equilibrium-binding constant (K_D (E)) values were calculated using a
546 nonlinear curve fit (y = (P1x)/(P2+x)). For the ILA1 TRBC1 TCR, single kinetic
547 injections were performed. For kinetics analysis, the K_{on} and K_{off} values were
548 calculated assuming 1:1 Langmuir binding and the data were analysed using a global
549 fit algorithm (BIAevaluation 3.1™).
550
551 **Cell staining and flow cytometry**
552
553 Flow cytometry was performed using BD LSR Fortessa instrument (BD, NJ, USA).
554 FACS sorting was performed using BD FACSAria (BD, NJ, USA). Staining steps were
555 performed at room temperature for 20 minutes, with PBS washes between steps. For
556 staining of intracellular antigens cells were fixed and permeabilised with 100uL of
557 Cytofix/ Cytoperm (BD, NJ, USA) for 5 minutes prior to staining, and wash steps were
558 performed using PermWash (BD, NJ, USA). The following antibodies were used (all
559 anti-human unless otherwise specified, clone identity in brackets): CD2 (TS1/8), CD3
560 (UCHT1), CD4 (OKT4), CD5 (UCHT2), CD7 (CD7-6B7), CD8 (SK1), human/ murine
561 CD11b (M1/70), CD14 (M5E2), CD19 (HIB19), CD25 (BC96), CD45 (HI30), CD45RA
562 (HI100), CD56 (HCD56), CD57 (HCD57), CCR7 (GO43H7), TCR α/β (T10B9), all from
563 Biolegend, San Diego, CA, USA; CD34 (Qbend10, Miltenyi, Bergisch Gladbach,
564 Germany); TRBC1 (JOVI-1, Ansell, Bayport, MN, USA), fixable viability dye
565 (eBioscience, ThermoFisher, Waltham, MA, USA). Anti-TRBC1 CAR expression was
566 detected by staining for RQR8 marker gene[22] with anti-CD34, or anti-MuFab (115-
567 116-072, Jackson Immuno, Westgrove, PA, USA). All antibodies other than JOVI-1
568 were validated by manufacturer for diagnostic use. At least 5000 target events were
569 acquired per sample. Analyses were conducted using FlowJo v10 (Treestar, Ashland,
570 OR, USA).
571
572
573 **Normal donors and viral peptide stimulation assays**
574
575 Approval for this study was obtained from the National Research Ethics Service,
576 Research Ethics Committee 4 (REC Reference number 09/H0715/64). All normal
577 donors provided informed consent.
578
579 PBMCs from unselected heathy donors were isolated by Ficoll-Paque (GE Healthcare,
580 Buckinghamshire, UK) gradient centrifugation were resuspended at 2 x 10^6 cells/ml
581 in 1ml complete media in wells of a 24-well plate. Overlapping peptide pools (15-mer,

11-mer overlap) derived from commonly immunogenic viral proteins were obtained from JPT Technologies (Berlin, Germany, USA). The viruses investigated (protein antigens in brackets) were cytomegalovirus, CMV (PP65) and adenovirus, AdV (hexon and penton). Peptide pools were supplied as dried pellets containing 25ug/peptide and were reconstituted in 50uL DMSO. To obtain a final concentration of 1ug/peptide/ml, 2ul of each peptide pool was added to each well of PBMCs.

After 1hr initial incubation, brefeldin A (BD, NJ, USA) was added to prevent Golgi transport. After a further 14hrs of culture, the cells were washed and surface staining was performed for viability, CD4 and CD8. The cells were then washed and lysed/ permeabilised, then stained for intracellular interferon-γ, CD3 and JOVI-1 before resuspension for FACS analysis. Negative control peptide pool (actin, a ubiquitous cytoskeletal protein) and positive control (PMA/ ionomycin, Sigma Aldrich, Darmstadt, Germany) conditions were included. Low-frequency viral-specific T-cells were identified by intracellular interferon-gamma expression, with positive response threshold set as >0.01% above negative control staining.

Identification of T-cell diiferentiation subsets and mucosal-associated invariate T-cells (MAITs) in normal donor peripheral blood

Cells were defined as: naïve (CD45RA+CD45RO-CCR7-CD62L-), central memory (CD45RA-CD45RO+CCR7+CD62L+), effector memory (CD45RA-CD45RO+CCR7-CD62L-) and effector (CD45RA-CD45RO+CCR7+CD62L+) and T-regulatory cells (CD4+FOXP3+CD25+). MAITs were identified as CD3+CD8+CD4-CD161+TCR-Vα7.2 +ve.

Invariant Natural Killer T-cell (iNKT) isolation

Peripheral blood mononuclear cells (PBMC) were isolated from healthy donor blood bags (Welsh Blood Service) using standard density gradient centrifugation. iNKT cells were purified from PBMC by magnetic separation using anti-iNKT TCR beads (Miltenyi Biotec) according to manufacturer's recommendations. The purified cell fraction was subsequently expanded with phytohaemagglutinin and allogeneic irradiated feeders from three donors. After a minimum of 14 days post expansion, cells were phenotyped and used in functional assays.

Molt-3 cell line (endogenously expressing CD1d) was pulsed overnight with 100 ng/ml α-galactosylceramide (αGalCer, Sigma). iNKT lines were subsequently co-incubated with Molt-3 pulsed with αGalCer for 5 hours in presence of monensin, brefeldin A and CD107a antibody (all from BD Biosciences), according to manufacturer's recommendations. iNKT lines were also incubated with media only, and with Molt-3 pulsed with vehicle only (DMSO). iNKTs were identified by upregulation of CD107a and IFN-γ in response to Molt-3 pulsed with αGalCer.

Retroviral transduction of T-cells

RD114-pseudotyped supernatant was generated as follows: 293T cells were transfected with vector plasmid; RDF, an expression plasmid to supply RD114 envelope (gift of Mary Collins, University College London); and PeqPam-env, a gagpol expression plasmid (gift of Elio Vanin, Baylor College of Medicine). Transfection was facilitated using Genejuice (Merck, Darmstad, Germany). Peripheral blood mononuclear cell transductions were performed as follows: T cells from normal donors were isolated by Ficoll (GE, Buckinghamshire, UK) gradient centrifugation and stimulated with phytohemagglutinin (Sigma Aldrich, Darmstadt, Germany) at 5mg/mL. Interleukin-2 (IL-2, Genscript, Nanjing, China) stimulation (100 IU/mL) was added following overnight stimulation. On day 3, T cells were harvested, plated on retronectin (Takara, Nojihigashi, Japan) and retroviral supernatant, and centrifuged at 1000g for 40 minutes. Transduction efficiency was determined on D6-7 following initial harvest and further experiments were commenced on D7-10 following initial harvest. PBMCs were maintained in complete RPMI.

Generation and cytotoxicity assessment of EBV-specific CTLs

This was performed as previously described[19]. Briefly, PBMCs from a normal donor were infected with EBV resulting in B-cell transformation to produce immortalised lymphoblastoid cells. These cells were irradiated and used as target cells to stimulate untransfomed PBMCs from the same donor, selectively expanding EBV-specific CTLs over a 23-day period. Cytotoxicity of EBV-CTLs against K562 cell line (an erythroleukaemia cell line with loss of MHC class 1 expression), allogeneic and autologous lymphoblastoid cells was assessed using standard 4hr chromium release cytotoxicity assays as previously described[39].

Preparation and staining of primary tumour samples for FACS or immunohistochemistry

Approval for this study was obtained from the National Research Ethics Service, Research Ethics Committee 4 (REC Reference number 09/H0715/64). Informed consent was obtained from all patients. For FACS, PBMCs from patients with T-cell malignancies were obtained from whole blood or marrow samples by Ficoll-Paque (GE Healthcare, Buckinghamshire, UK) gradient centrifugation prior to staining and analysis as above. Gating strategies to identify tumour and healthy T-cells were determined on a patient-specific basis according to data previously obtained by primary clinical laboratories. For immunohistochemistry, fresh biopsy samples of patients with a range of T-cell malignancies (see Figure 3f) were snap-frozen in liquid nitrogen and tissue sections were prepared according to standard methodology. The investigated antibodies included the mouse monoclonal anti-T Cell Receptor Beta 1 (clone JOVI.1; Ancell Corporation, Bayport, MN, USA) and the mouse monoclonal anti-TCR beta F1 (clone 8A3; Thermo Fisher Scientific, Loughborough, UK). The antibodies were assessed under different conditions (i.e. dilution and antigen retrieval protocol) and the chosen dilution which showed selective background-free reaction in fresh tissue sections of human reactive tonsils (nr. 2) used as positive control were 1:5000 for JOVI.1 and 1:50 for TCR Beta F1 respectively. The staining procedure was performed using the Roche-Ventana BenchMark Ultra autostainer (Ventana Medical System, Tuscon, US). Counterstaining was performed using haematoxylin and bluing reagent from Ventana/Roche; slides were mounted with cover slips and air-dried.

Chromium release cytotoxicity assays

Standard 4hr chromium release cytotoxicity assays were performed as previously described[39], with all assays performed in triplicate. NK cell depletion was performed prior to assays using CD56 magnetic bead depletion and LD columns (Miltenyi, Begisch Gladbach, Germany).

FACS-based co-culture and cytotoxicity assays

Target and effector cells were resuspended at 1M cells/ml in complete media. 50-100uL of each cell suspension was added to wells of a V-bottom 96-well plate to

achieve a 1:1 E:T ratio with 50 000 or 100 000 targets/ well. For some experiments target cell were pre-labelled with carboxyfluorescein succinimidyl ester (CFSE) or CellTrace Violet (CTV, both Invitrogen, Carlsbad, CA, USA) dyes according to manufacturer's instructions. The plate was placed in a standard cell culture incubator containing 5% CO_2 at 37°C. After 24hrs the plate was spun down at 400G for 5mins, 100uL of supernatant was removed for cytokine assays and replaced with fresh complete media. At 48hrs or 7 days, the plate was spun down at 400G for 5mins and supernatant was decanted. 100uL of staining cocktail (appropriate antibodies/ viability dye (eBioscience, ThermoFisher, Waltham, MA, USA) diluted in PBS) was added and cells were stained for 20mins in the dark at room temperature. Wells were then washed with a further 100uL of PBS and spun down at 400G for 5 mins. Supernatant was decanted. Counting beads (Flow check fluorospheres, BD, NJ, USA) were washed in PBS then resuspended at 100 000 beads/ ml in PBS. 100uL of PBS/ counting bead mixture was added to each cells (10 000 beads/ well). 2000 beads were acquired per sample. Gating on single live target cells was performed according to exclusion of fixable viability dye, forward and side scatter characteristics and expression of fluorescent protein, marker gene or fluorescent dye. Assays were performed in triplicate. % cytotoxicity was calculated as: 10000/ number of beads collected x number of target cells at end/ number of target cells at start of culture x 100.

For primary tumour killing experiments, allogeneic or autologous T-cells were used, depending on the availability of cryopreserved normal patient T-cells. Bespoke gating strategies were used to identify normal and malignant T-cells in each patient sample.

Cell sorting with magnetic bead selection

Transduced T-cells positive or negative for the RQR8 marker gene (contains Qbend10-CD34 epitope) were selected by positive or negative bead selection according to the manufacturer' instructions (Miltenyi, Miltenyi, Bergisch Gladbach, Germany) using MS or LD columns respectively. For TRBC1 T-cell positive or negative selection, cells were initially stained with JOVI-1-biotin then incubated with streptavidin-conjugated magnetic beads, then separated according to the manufacturer's instructions. To increase purity a second selection/ depletion round was performed.

Murine models of T-cell malignancy

This work was performed under United Kingdom home-office–approved project license and was approved by University College London Biological Services Ethical Review Committee. 6-8 week old male non-obese diabetic-severe combined immunodeficiency γ-chain–deficient (NSG) mice (Jackson Laboratory, Bar Harbor, ME, USA) were intravenously injected via the tail vein with tumour cells, human PBMCs or CAR T-cells as described in the text. An otherwise identical irrelevant control CAR targeting B-cell maturation antigen, which is not expressed in T-cell malignancies, was used in some experiments as indicated in the text. Tail vein bleeds of 50uL were undertaken as indicated in the text. At the time of cull, in some experiments bone marrow was harvested. Single cell suspensions were prepared and analysed for presence of T-cells and residual tumour by flow cytometry. Tumour cells were identified by CD19 or BFP marker gene according to experiment. CAR T-cells were identified by expression of RQR8 marker gene.

For experiments with a survival endpoint or engraftment of PBMCs, mice were monitored with at least twice weekly weighing. Animals with >10% weight loss or those displaying evidence of GvHD or tumour progression including hunched posture, poor coat condition, reduced mobility, pilorection or hind limb paralysis were culled.

Bioluminescent imaging of mice was performed using IVIS system (Perkin Elmer, Buckinghamshire, UK). Prior to imaging, animals were placed in an anesthetic chamber. General anesthesia was induced using inhaled isoflurane. Following induction, intraperitoneal injection of luciferin (200uL via 27G needle) was undertaken. After 2 minutes, mice were placed in the imaging chamber. Simultaneous optical and bioluminescent imaging was performed. Anaesthesia was maintained by continued inhalation of isoflurane during imaging.

Statistical analyses

Unless otherwise noted, data are summarised as mean ± SEM. Student's *t*-test was used to determine statistically significant differences between samples for normally distributed variables, with Mann-Whitney U-test used for non-parametrically distributed variables. $p < 0.05$ (2-tailed) indicated a significant difference. Unless otherwise stated, variances were similar between study populations. When variances were unequal, Welch's correction for unequal variance was used. Paired analyses were used when

appropriate. When 3 groups were compared, 1-way ANOVA with Dunnett's test for multiple comparisons with alpha of 0.05 were used. When multiple t-tests were performed, statistical significance was determined using the Holm-Sidak method with alpha of 0.05. Neither randomisation nor blinding was done during the *in vivo* study. However, mice were matched based on the tumor signal for control and treatment groups before infusion of control or gene-modified T-cells. Cohort sizes were based on number required to demonstrate 90% reduction in tumour bioluminescence, 95% confidence with 80% power. Survival curves were generated using the Kaplan-Meier method with hazard ratios calculated by Mantel-Haenszel method. All animal studies were performed at least twice, with data presented representing one representative experiment. Graph generation and statistical analyses were performed using Prism version 7.0b software (GraphPad, La Jolla, CA, USA).

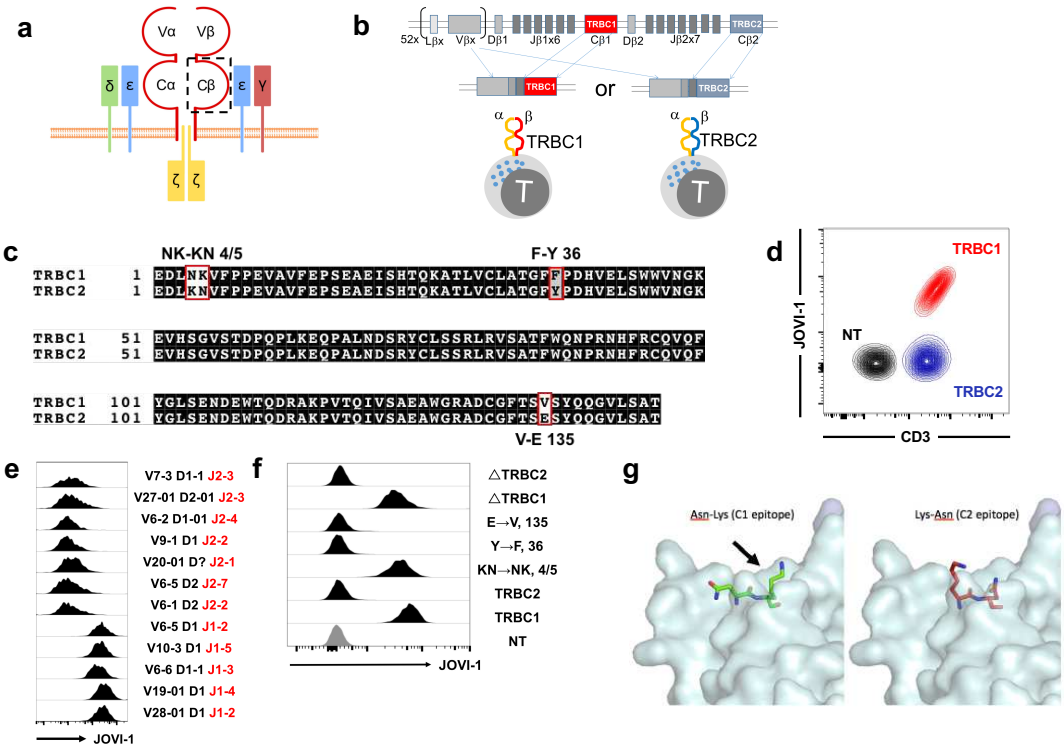

Figure 1: During T-cell receptor gene re-arrangement, each T-cell selects either TRBC1 or TRBC2, which can be specifically differentiated using an antibody. (a) Proposed structure of the TCR-CD3 complex assembled on T-cell surface (beta constant region highlighted) (b) The process of beta gene arrangement involving specific VDJ recombination (c) Alignment of TRBC1 and TRBC2 protein sequences, differences highlighted in red (d) Staining of non-transduced and engineered TRBC1-JKO, TRBC2-JKO cell lines with CD3 and JOVI-1 antibodies (e) JOVI-1 staining of 293T cells, transfected to express TCRs with varying specificities and TRBJ usage (gated on CD3+ cells) (f) JOVI-1 staining of engineered cell lines with each difference between TRBC1 and TRBC2 introduced individually (g) 3D representation of TRBC1 and TRBC2 epitopes on the surface of TRBC. TCR = T-cell receptor; VDJ = variable, diversity, joining; JKO = Jurkat T-Cell receptor knockout. TRBC = T-cell receptor beta constant.

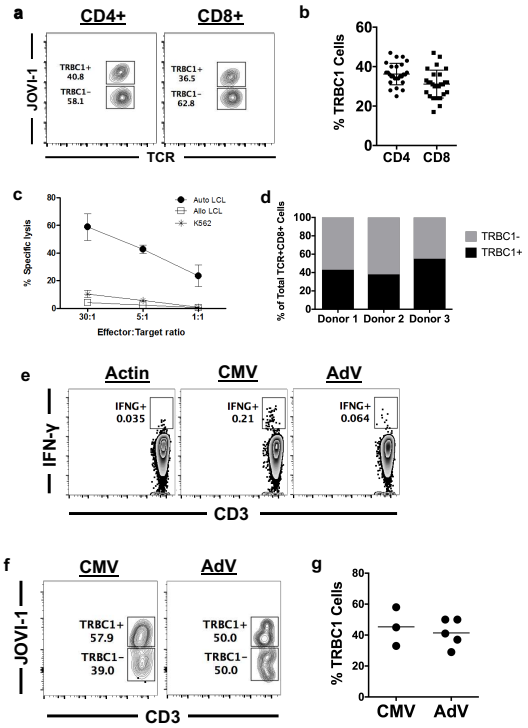

Figure 2: Unselected polyclonal and viral-specific T-cells contain both TRBC1+ and TRBC1- populations. (a) Staining of sample normal donor CD4 (left) and CD8 (right) T-cells with pan-TCR and JOVI-1 antibodies (b) Proportion of normal T-cells expressing TRBC1 in CD4 and CD8 compartments, data from 27 normal donors. (c) Killing of cell lines by EBV-CTLs, measured by 4hr chromium release assay (d) TRBC1+/TRBC1- proportion of EBV-CTLs in 3 normal donors (e) Identification of CMV or AdV-specific T-cells by IFN-G staining after peptide stimulation, data from representative donor (f) Staining of viral specific T-cells with CD3 and JOVI-1 (gated on cells as identified in e) (g) TRBC1 expression in viral specific cells, summary data from 3 (CMV) and 5 (AdV) normal donors. TCR = T-cell receptor, EBV = Epstein Barr virus, CTL = cytotoxic T-lymphocyte, CMV = cytomegalovirus, AdV = adenovirus, IFN-G = interferon gamma.

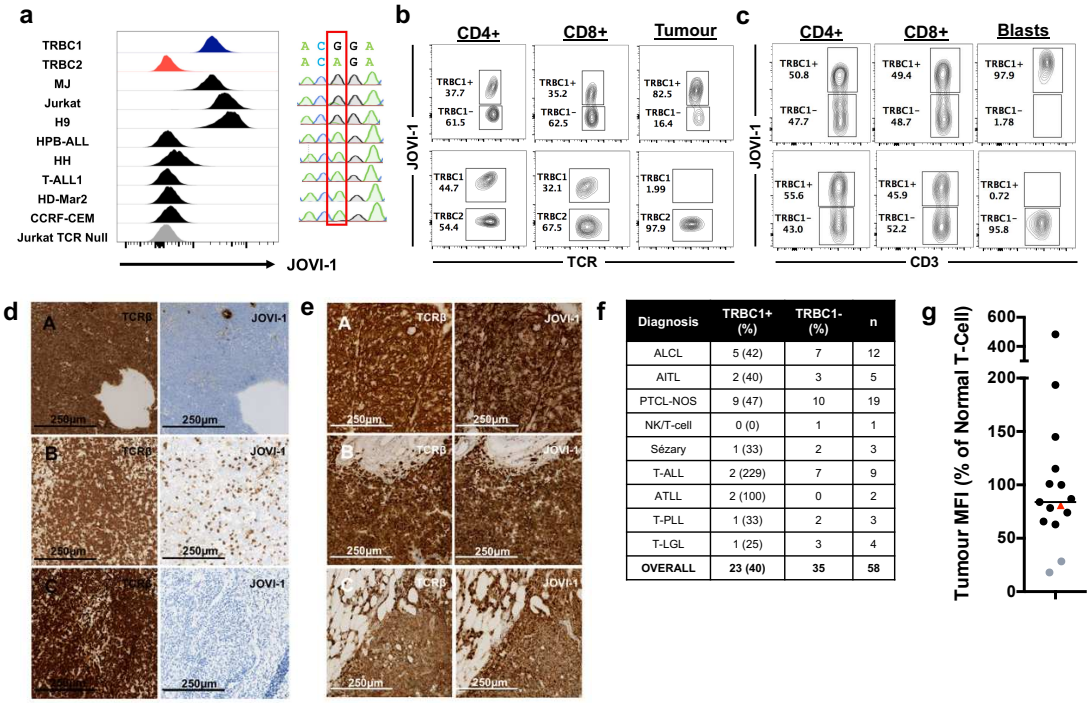

Diagnosis	TRBC1+ (%)	TRBC1- (%)	n
ALCL	5 (42)	7	12
AITL	2 (40)	3	5
PTCL-NOS	9 (47)	10	19
NK/T-cell	0 (0)	1	1
Sézary	1 (33)	2	3
T-ALL	2 (229)	7	9
ATLL	2 (100)	0	2
T-PLL	1 (33)	2	3
T-LGL	1 (25)	3	4
OVERALL	**23 (40)**	**35**	**58**

Figure 3: T-cell-derived cell lines and primary T-cell malignancies are clonally TRBC1+ or TRBC1-. (a) Staining of cell lines with JOVI-1 (left panel), gated on CD3+ cells with matched Sanger sequencing traces of TCR-beta constant region (right panel) (b) Staining of normal and malignant T-cells from 2 representative patients with T-LGL, assessed by flow cytometry. Top panel shows TRBC1+ tumour, bottom panel shows TRBC1- tumour. Tumour gating = TCR+CD4-CD8+CD57+ Small numbers of TRBC1- cells in tope panel 'tumour' gate likely reflect normal CD8+CD57+ T-cells, clonality suggested by abnormal TRBC1+:TRBC1- ratio (c) Staining of normal and malignant T-cells from 2 representative patients with T-ALL, assessed by flow cytometry. Top panel shows TRBC1+ tumour, bottom panel shows TRBC1- tumour. Tumour gating = CD3(intra)+CD4+CD8+. (d) Staining of frozen tissue sections of 3 cases of TCR+ TRBC1- lymphoma with TCR (left panel) and JOVI-1 (right panel). Positive cells stain brown. Small numbers of admixed polyclonal TRBC1+ T-cells are typically seen. Tumour histology: A = T-acute lymphoblastic leukaemia (T-ALL), B = angioimmunoblastic T-cell lymphoma (AITL), C = AITL (e) Staining of frozen tissue sections of 3 cases of TCR+ TRBC1+ lymphoma with TCR (left panel) and JOVI-1 (right panel). Positive cells stain brown. A = anaplastic large cell lymphoma (ALCL), B = T-ALL, C = peripheral T-cell lymphoma not otherwise specified (PTCL-NOS) (f) Summary data of TRBC1 expression in primary samples of TCR+ malignancies. (g) TCR expression on tumour cells and TRBC1+ cell lines. Tumour expression of TCR

was quantified by MFI on FACS, and is expressed as a percentage of TCR expression on admixed normal T-cells from the same patient. Grey triangles represent cases of ATLL, with other histologies represented by black circles. Red triangle = Jurkat cell line. T-LGL = T-large granular lymphocytosis, T-ALL = T-acute lymphoblastic leukaemia, AITL = angioimmunoblastic lymphoma, ALCL = anaplastic large cell lymphoma, NK = natural killer, ATLL = adult T-cell leukaemia/ lymphoma, T-PLL = T-prolymphocytic leukaemia. MFI = median fluorescence intensity.

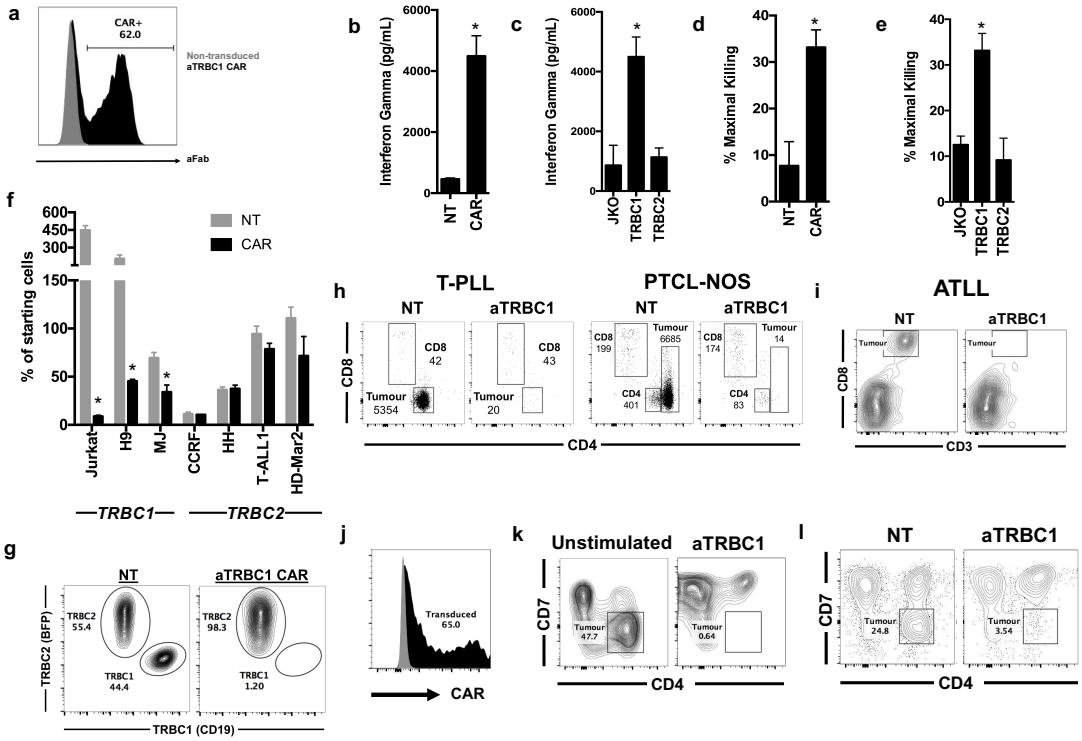

Figure 4: Anti-TRBC1 CART-cells demonstrate efficacy and specificity against TRBC1+ tumours *in vitro*. (a) Example transduction shows anti-TRBC1 CAR expression on surface of transduced T-cells. (b) Interferon gamma release by NT or anti-TRBC1 CAR T-cells against TRBC1-JKO cells, 24-hour co-culture. (c) Interferon gamma release by anti-TRBC1 CAR T-cells against NT-JKO, TRBC1-JKO or TRBC2-JKO cells, 24-hour co-culture. (d) Killing of TRBC1-JKO cells by NT or anti-TRBC1 CART-cells, 4hr chromium release assay. *p<0.01 for comparison v NT effectors. (e) Killing of TRBC1-JKO or TRBC2-JKO cells by anti-TRBC1 CART-cells, 4hr chromium release assay *p<0.01 for comparison v JKO-NT target cells. (f) Flow-based cytotoxicity assay, target cell numbers expressed as % of starting cells after 48hrs. (g) Co-culture of mixed TRBC1/ TRBC2 cells, example FACS plot at 48hrs. (h) Primary T-cell malignant samples with admixed normal CD8 T-cells after 120hr co-culture with NT or anti-TRBC1 allogeneic CAR –cells. Left panel = case of T-PLL, tumour cells were CD7bright CD4+. There were no normal CD4 cells but normal CD8 cells were present. Right panel = PTCL-NOS. Numbers represent % of events. Tumour cells were CD4brightCD7-. Normal admixed CD4 and CD8 cells were present. Numbers represent absolute numbers of events. (i) Primary ATLL sample after 72hr co-culture with allogeneic NT or anti-TRBC1 CAR T-cells. Tumour cells were CD3dimCD8+CD7-. Numbers represent % of events. (j) Transduction of PBMCs from patient with ATLL, assessed by RQR8 marker gene. Grey = NT cells, black = anti-TRBC1. (k) Tumour

burden following transduction with anti-TRBC1 CAR. (l) Primary ATLL sample after 72hr co-culture with autologous NT or anti-TRBC1 T-cells. Tumour gating = CD2+CD4+CD7-CD8-. All experiments other than in j-l used effector T-cells from normal healthy donors. NT = non-transduced, JKO = Jurkat T-cell receptor-null, CAR = chimeric antigen receptor, BFP = blue fluorescent protein, ATLL = adult T-cell leukaemia/ lymphoma, T-PLL = T-prolymphocytic leukaemia, PTCL-NOS = peripheral T-cell lymphoma, not otherwise specified.

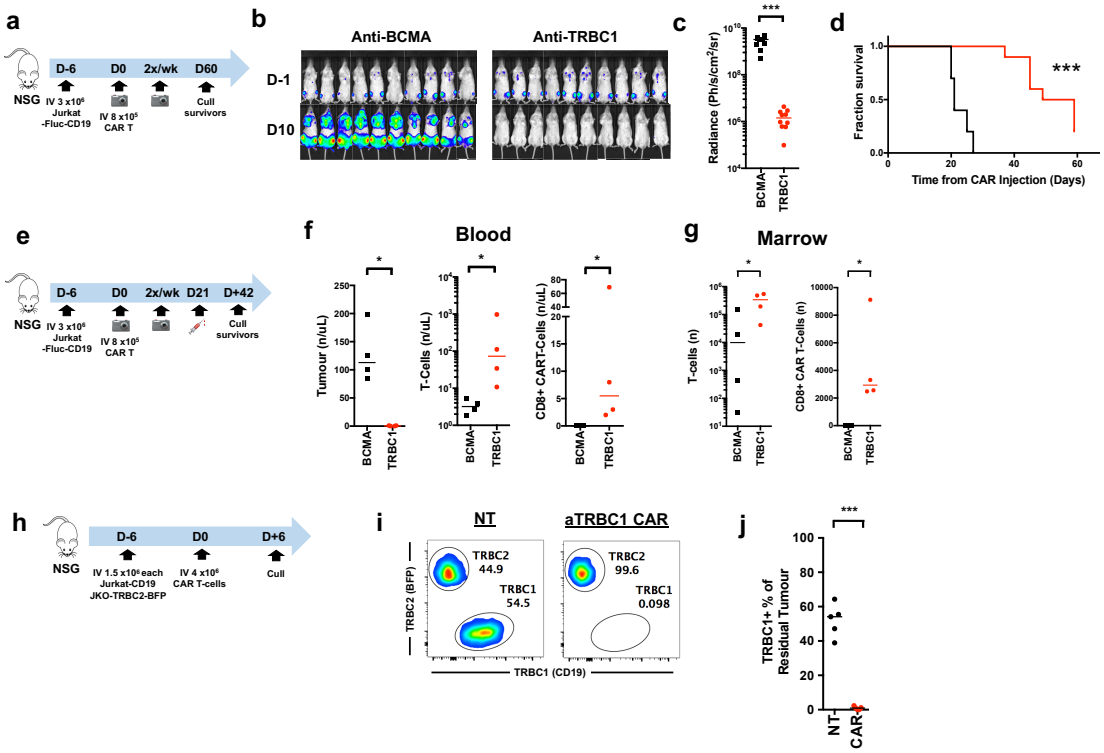

Figure 5: Efficacy and specificity of anti-TRBC1 CAR in murine models of TRBC1+ malignancy. (a) Flow diagram of Jurkat survival experiment (b) Bioluminescence imaging at D-1 and D10 following CAR injection (c) Radiance of individual animals at D10 following CAR injection, compared via Student's t-test (d) Survival curve of animals in Jurkat experiment (median OS 54 v 21 days, HR = 0.037, $p < 0.00001$, n = 10/ group) (e) Flow diagram of Jurkat persistence experiment (f) Jurkat tumour, total T-cell and CD8 CAR-T cell numbers from bleed at D21 following CAR injection (g) Numbers of total T-cells and CD8 CAR T-cells in marrow at time of cull (D42 in anti-TRBC1 CAR recipients). Comparisons in f,g were made using Mann-Whitney U-test. CAR was detected by expression of RQR8 marker gene (h) Flow diagram of specificity experiment (i) Flow cytometry of bone marrow in NSG mice engrafted with equal proportions of TRBC1-Jurkat or TRBC2-JKO cells following treatment with NT effectors or anti-TRBC1 CART-cells, representative examples. TRBC1 cells were detected by CD19 marker gene, TRBC2 cells were detected by BFP marker gene) Quantification of TRBC1 proportion of residual Jurkat tumour by flow cytometry, individual values shown. All experiments used effector T-cells from normal healthy donors. Comparison by Student's t-test. Horizontal lines represent median values.

*p<0.05, ***p<0.00001. BCMA = B-cell maturation antigen. BFP = blue fluorescent protein.

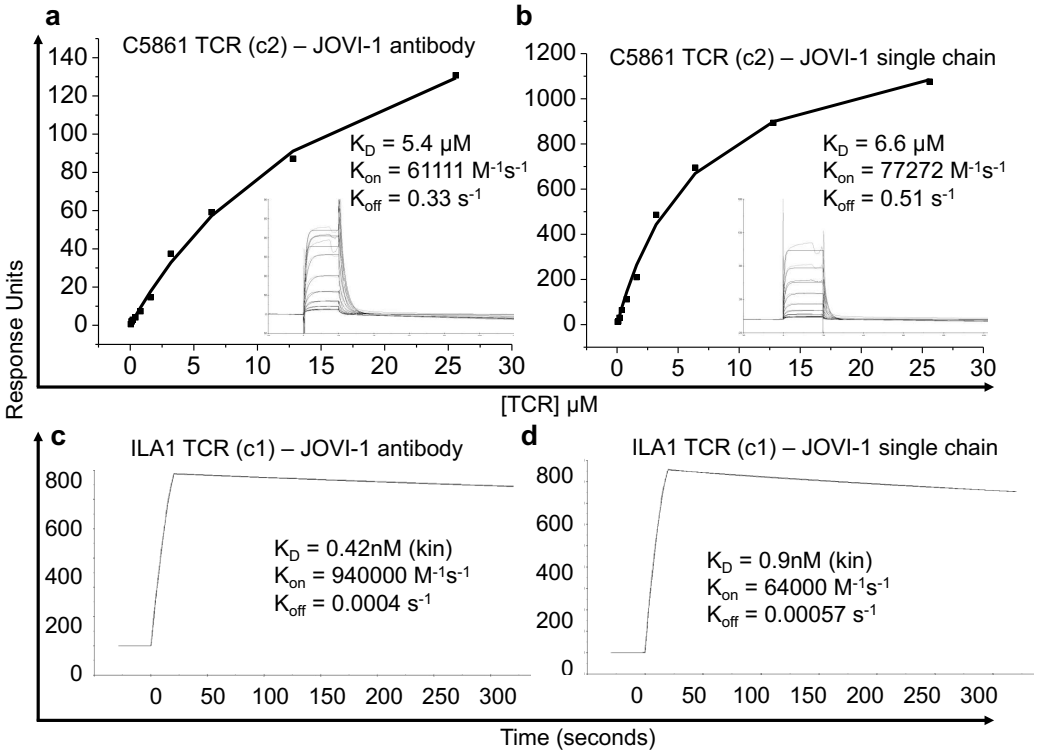

Supplementary Figure 1: Surface plasmon resonance data of JOVI-1 binding to TRBC1 and TRBC2 TCR protein. JOVI-1 antibody (a) and single chain variable fragment (ScFv) (b) binding to C5861 (TRBC2) TCR protein. JOVI-1 antibody binding (c) and ScFv binding (d) to ILA1 (TRBC1) TCR. TCR = T-cell receptor, ScFv = single chain variable fragment. Top row = plots demonstrating TCR concentration v peak response units for binding to TRBC2 TCR, with time v response units plots at varying concentrations of TCR inset. Bottom row demonstrates time v response units plots for binding to TRBC1 TCR.

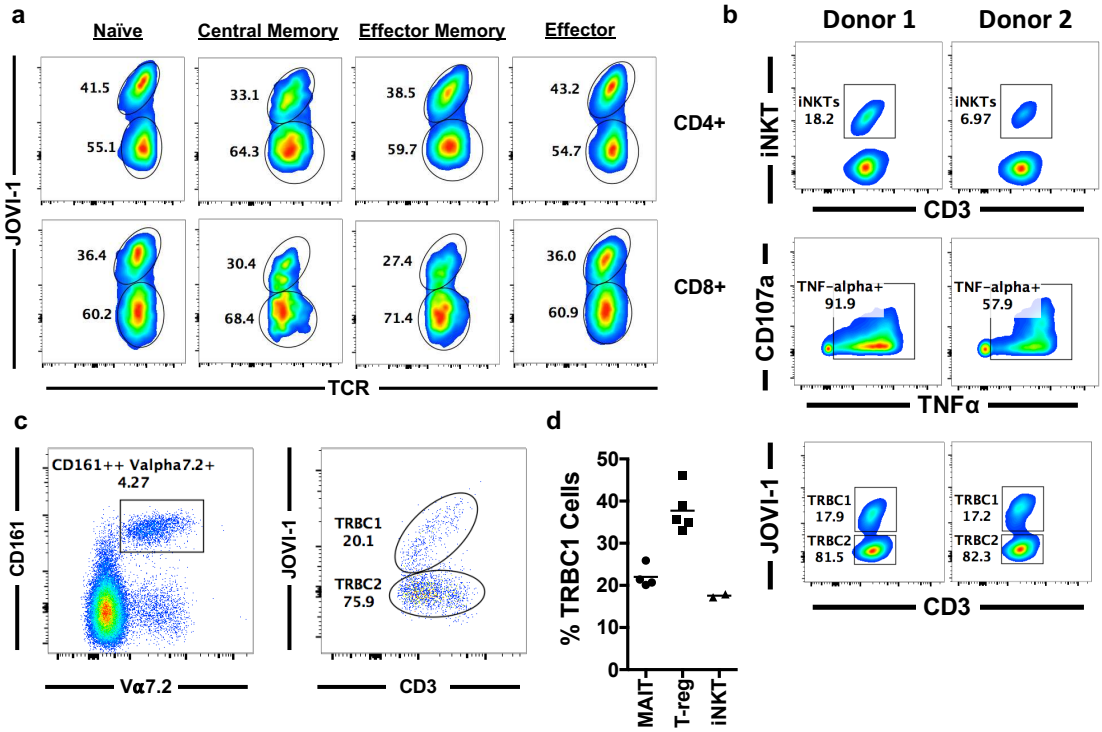

Supplementary Figure 2: TRBC1 expression in T-cell subsets. (a) Naïve (CD45RA+CD45RO-CCR7-CD62L-), central memory (CD45RA-CD45RO+CCR7+CD62L+), effector memory (CD45RA-CD45RO+CCR7-CD62L-) and effector (CD45RA-CD45RO+CCR7+CD62L+) were identified by FACS. Staining with TCR and JOVI-1 antibodies demonstrated each T-cell population contained both TRBC1+ and TRBC1- cells. Data from 1 donor shown, repeated in 4 donors. (b) iNKT cell lines were produced as described in Methods section. Cells were CD3+Valpha24Jalpha18+ (top row) and expressed TNF-alpha and CD107a in response to Molt-3 cells pulsed with αGalCer (middle row, gated on iNKTs). Cells expressed both TRBC1+ and TRBC1- TCRs (bottom row, gated on iNKTs). (c) MAITs were identified as CD3+CD8+CD161brightValpha7.2 cells (left panel) and contained both TRBC1 and TRBC2 cells (right panel) (d) Summary data of TRBC1 expression in T-cell populations. TCR = T-cell receptor, MAIT = mucosal-associated invariant T-cells, iNKT = invariant natural killer/ T-cells.

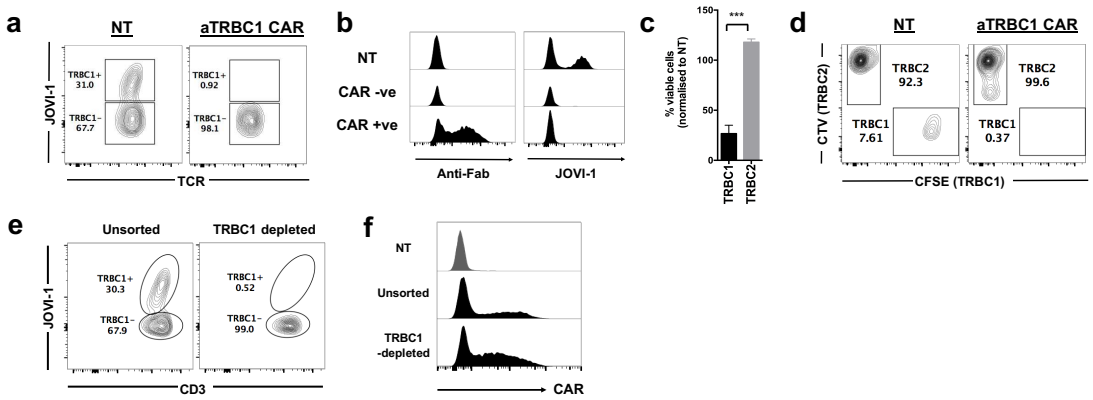

Supplementary Figure 3: Epitope blocking and primary T-cell cytotoxicity assay using anti-TRBC1 CAR. a) NT cells (left) and anti-TRBC1 CAR-transduced cells (right) stained with TCR and JOVI-1 antibodies, representative example, donor n > 10. b) Anti-TRBC1 CAR T-cells sorted into CAR-ve and CAR +ve fractions by CD34 magnetic sort, stained with anti-murine Fab antibody (left panel) or JOVI-1 antibody (right panel). Representative example, repeated x 3 c) Killing of fluorescently labelled primary TRBC1 or TRBC2 T-cells in 1:1 co-culture with autologous non-transduced or anti-TRBC1 CART-cells, FACS at 7 days, n = 3, ***p<0.001, unpaired t-test anti-TRBC1 CAR v NT effectors. d) Co-culture with CFSE-labelled TRBC1 and CTV-labelled TRBC2 cells, mixed at 1:2 ratio and incubated with autologous NT or anti-TRBC1 CAR T-cells, flow cytoemetry at 7 days, 1 representative donor shown, donor n = 3. e) Example of purity of TRBC1-depleted T-cells f) Transduction of unsorted or TRBC1-depleted T-cells with anti-TRBC1 CAR, transduction assessed by blue fluorescent protein marker gene. 1 representative donor shown, repeated in >3 donors. All experiments used T-cells from normal healthy donors. NT = non-transduced, CAR = chimeric antigen receptor, CFSE = carboxyfluorescein, CTV = Cell Trace Violet

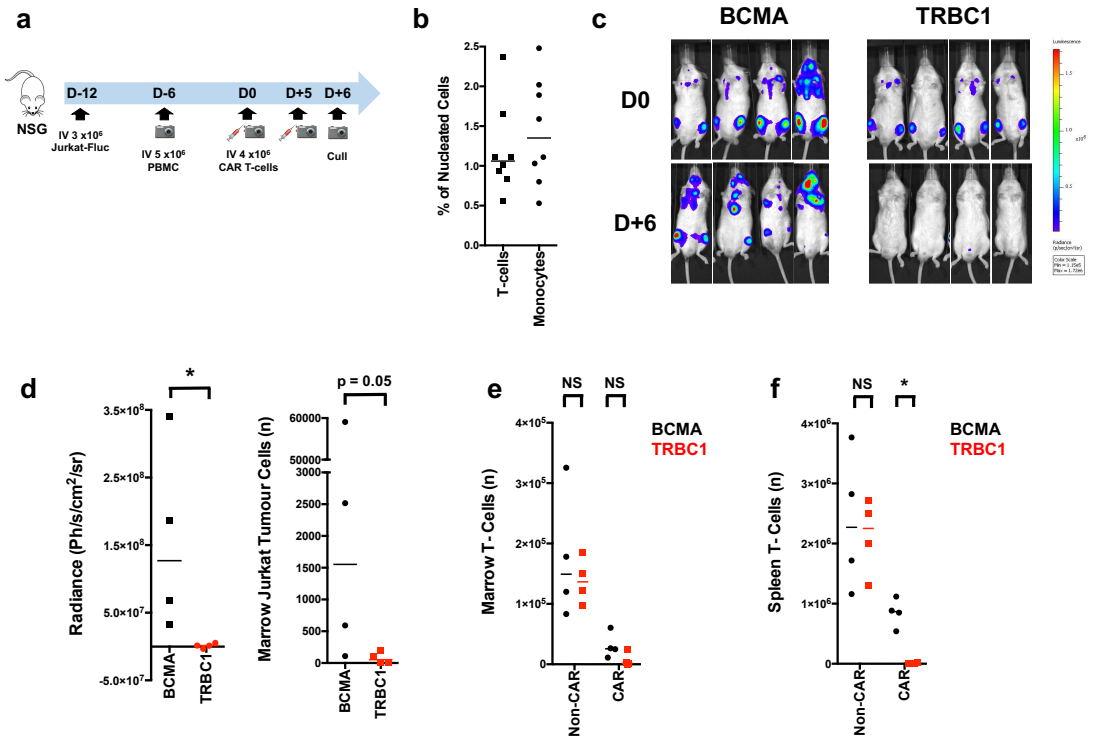

Supplementary Figure 4: Efficacy of anti-TRBC1 CAR against TRBC1+ Jurkat tumour in human PBMC-engrafted mouse model. (a) Flow diagram of experiment (b) Engraftment of human peripheral blood cells at D6 following PBMC injection (c) Bioluminescence imaging of Jurkat tumour at D0 and D+6 following CAR injection (85% CAR+) (d) Quantification of residual Jurkat tumour by bioluminescence imaging (left) and flow cytometry of bone marrow (right). No Jurkat cells were present in spleens of either group. (e) Quantification of normal non-Jurkat T-cells in marrow. (f) Quantification of normal non-Jurkat T-cells in spleen. Anti-BCMA CAR-treated mice = black, anti-TRBC1 CAR-treated mice = red. PBMCs and effector T-cells were derived from the same healthy donor. Human monocytes were identified as CD45+CD3-CD19-CD11b+. Jurkat tumour cells were identified as CD45+CD3+CD19+CD4dim, normal T-cells were identified as CD45+CD3+CD19-RQR8-CD4+CD8- or CD45+CD3+CD19-RQR8-CD4-CD8+, and CAR T-cells were identified as CD45+CD3+CD19-RQR8+. * $p < 0.05$. Horizontal lines represent median values. All statistical comparisons used Mann-Whitney U-test. PBMC = peripheral blood mononuclear cells, CAR = chimeric antigen receptor, BCMA = B-cell maturation antigen. NS = non-significant